

Radio-frequency size effect in a layer of normal metal bounded by its superconducting phase

I. P. Krylov and Yu. V. Sharvin

Institute for Physics Problems, U.S.S.R. Academy of Sciences

(Submitted October 23, 1972)

Zh. Eksp. Teor. Fiz. 64, 946-957 (March 1973)

The radio-frequency size effect (RFSE) is investigated in a layer of a normal metal bounded by its superconducting phase and a vacuum. It is shown experimentally that the excitations are reflected from the boundary between the phases with momentum conservation and sign reversals of the velocity vector, charge, and mass, in agreement with Andreev's theory. This is confirmed both by the observation of first-order RFSE lines when the normal-layer thickness equals half the diameter of the extremal trajectories and by the shapes of the second-order RFSE lines. The latter differ from the line shape in a normal-metal plate only with respect to the sign of the signal. By varying the thickness of the normal-metal layer it was possible to measure the electron mean free paths in different extremal cross sections.

1. INTRODUCTION

By measuring the surface impedance of metals characterized by a large electron mean free path l in magnetic fields it can be learned what fraction of the surface conductivity is contributed by electrons that return to the skin layer after moving in orbits having dimensions of the order of l . Thereby it becomes possible to obtain information about processes occurring in a metal at a considerable distance from a surface that is exposed to radio-frequency radiation. In the cases of plates with thicknesses $d \lesssim l$ the interaction of the electrons with the opposite boundary of a sample leads to several radio-frequency size effects (RFSE) that have been studied intensively in recent years (see the review^[1], for example).

It is obvious, however, that this method can also be used, in principle, to investigate the interactions of electrons with any inhomogeneities in the structure of a metal. We have published a preliminary communication^[2] concerning the discovery of a new type of RFSE which appears with the reflection of electrons from the boundary between the normal (n) and superconducting (s) phases of a metal. We shall here present the results obtained from a more thorough investigation of this effect. Interest in this work is associated with the distinctive character of the reflection of carriers (electrons and holes) in a normal metal from the n-s boundary. Andreev was the first to show^[3] that a transition layer having thickness of the order of the coherence length $\xi \approx 10^{-4}$ cm is too "weak" a barrier to cause ordinary reflection of an excitation wherein the change of the momentum \mathbf{p} is of the order of the Fermi momentum $p_f \approx 10^{-19}$ g-cm/sec. However, excitations with energies $\epsilon = |v(\mathbf{p} - \mathbf{p}_f)|$ (reckoned from the Fermi level ϵ_f ; v is the velocity of the excitation) cannot penetrate into the superconducting phase because usually $\epsilon \ll \Delta$, which is the energy gap in the excitation spectrum of a superconductor. For this situation Andreev suggested that in reflection from the n-s boundary the momentum of the excitation is practically conserved, changing by only the amount $\Delta p \sim \epsilon/v$. At the same time, however, the character of the excitation changes: an electron is converted into a hole and vice versa. In virtue of the central symmetry of the dispersion law, $\epsilon(\mathbf{p}) = \epsilon(-\mathbf{p})$, the sign of the velocity vector $\mathbf{v} = \partial\epsilon/\partial\mathbf{p}$ of the excitation is reversed. Since the signs of the

charge and effective mass are also simultaneously reversed, the density of the current flowing from the normal to the superconducting phase can differ from zero, but the direction of the Larmor precession of the carriers in a magnetic field remains unchanged (Fig. 1). The probability of reflection is obviously unity for excitations with $\epsilon \leq \Delta$.

Measurements of the integral properties of the intermediate state (thermal conductivity, specific heat, and electric conductivity) confirm Andreev's theory, as does the direct observation of electron reflection from the n-s boundary by means of the RFSE.^[2] Let us consider the RFSE mechanism in the n-layer. When the n-layer thickness d is sufficiently larger than the dimensions D of extremal electron orbits (Fig. 2a), the surface impedance $Z = R + iX$ has the value obtained for a semi-infinite metal. As d decreases, electrons returning to the skin layer begin to be reflected from the n-s boundary (Fig. 2, b and c, where the reflection-induced sign reversal of the charge is depicted by changing from a solid to a dashed curve and vice versa). When the dashed parts of the trajectory begin to traverse the skin layer (Fig. 2c) they make a negative contribution to the surface current. We can thus expect that the curve representing the dependence of Z on the thickness of the n-layer will exhibit singular behavior when the equality $d = D/2$ is satisfied. Size effects of a higher order are also possible at larger values of d . It is known^[1] that in a normal metal at depths which are multiples of D "spikes" of the electromagnetic field and of the current appear. Passage of the n-s boundary through the spike region induces a change of the field distribution in the spike. Because of electrons passing through the spike and returning to the skin layer, the changed structure of the spike affects the surface impedance and should lead to the appearance of RFSE lines at $d = mD/2$ (m is an integer). The intensity of these lines should evidently fall off as m increases.

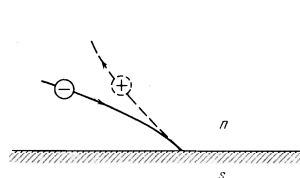


FIG. 1

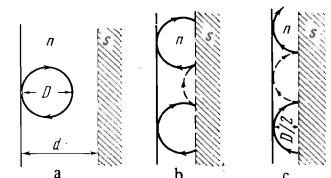


FIG. 2

It should be noted that the line for $d = D/2$ and also other higher-order "half-integer" lines would be absent in the cases of both diffuse and specular electron reflection from the layer boundary.

2. EXPERIMENT

A uniform n-layer and a geometrically regular n-s boundary can be obtained using an inhomogeneous magnetic field H . If a sufficiently high direct current is sent through a conductor that lies along the axis of a hollow cylindrical sample, on the inside surface of the cylinder a layer of normal metal will appear with a thickness that depends on the strength of the current (Fig. 3). For a cylinder of inside radius $a \gg D$ the inhomogeneity of the field does not lead to appreciable distortions of the electron trajectories in comparison with the case of a homogeneous field. The dimension D of a trajectory in the radial direction for a central cross section of a Fermi surface having any shape is given, with accuracy $\sim (D/a)^2$, by the usual equation $2p = eHD/c$, where $2p$ is the dimension of the cross section in the axial direction in momentum space, and H is the field strength at the average distance \bar{r} from the axis: $\bar{r} = (r_{\max} + r_{\min})/2$. Inhomogeneity of the field leads to a small electron drift along the cylinder axis; the displacement is $\sim (D/a)^2$ per cyclotron period. This relationship and the equality $H = H_c$ (the critical field) at the n-s boundary enable us easily to relate the current I at which we observe the RFSE ($m = 1$) line for the cross section of extremal dimension $2p$, to the current I_c that flows when the field at the inside surface of the sample equals H_c :

$$(I - I_c) / I_c = d/a \approx (pc/eH_c a)(1 - pc/2eH_c a) \quad (1)$$

where the approximate equality is correct to terms of the order $\sim (d/a)^3$. It is easily seen that for extremal cross sections of a Fermi surface that is convex in the direction of the cylinder axis, the condition $d = D/2$ will be satisfied with relative accuracy $\sim (D/a)^2$, independently of the rotation angle around the cylinder axis, while the corresponding orbit exists.

It follows from (1) that the difference $I - I_c$ is independent of temperature in first approximation, while I_c varies with H_c . It should also be noted that I_c does not coincide with the current I_c' at which the n-layer appears on the inside surface. This difference $\Delta I = I_c - I_c'$ results from the existence of the surface energy $\xi H_c^2/8\pi$ of the n-s boundary. From the principle of minimum free energy of the system it is computed thermodynamically that an equilibrium n-s boundary appears at the distance $\sqrt{\xi}a$ from the cylinder surface when $\Delta I/I_c \approx \sqrt{\xi}/a$ (corrections $\sim \xi/a$ can be neglected).

Samples. Single-crystal samples of 99.9999% pure

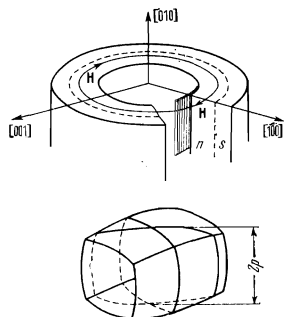


FIG. 3. Relative orientations of the field, hf coil, and a part of the Fermi surface (below).

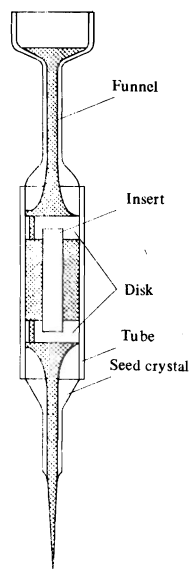


FIG. 4

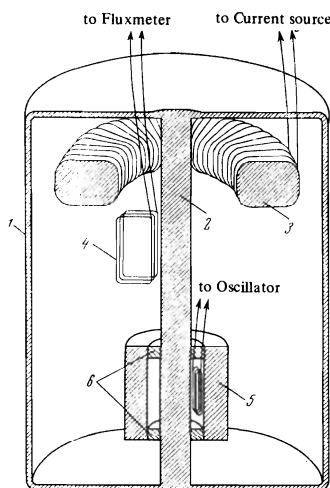


FIG. 5

FIG. 4. Device for preparing the samples.

FIG. 5. Schematic drawing of experimental apparatus.

tin, about 12 mm in diameter and 15 mm long, were cast in a glass tube (Fig. 4). A cylindrical rock salt insert of 6.20-mm diameter was secured along the tube axis by means of glass disks. The insert was shaped on a lathe and was polished with silk cloth in a 96% alcohol solution. The insert deviated at most 1μ from a geometrically perfect right circular cylinder. The metal was poured through a funnel; a seed crystal provided for the needed crystal orientation. For the purpose of testing the reproducibility of the experimental effects three samples of approximately identical orientation were grown with their [100] axis along the cylinder axis. The data given in the present paper were obtained from a sample whose [100] axis deviated $\leq 1^\circ$ from the cylinder axis. Rock salt was chosen as the material of the insert in order to guarantee its removal without damaging the sample, by dissolving the salt in water. However, the thermal expansion coefficients of the salt and tin are so different that the insert could simply be drawn out without appreciably damaging the inside surface.

Since the thermal expansion of tin is anisotropic, the cross section of a sample having its tetragonal [001] axis perpendicular to the cylinder axis acquires an elliptic shape upon cooling. Using the known thermal expansion coefficients of rock salt^[4] and tin,^[5] we computed the semiminor axis $b = 3.07$ mm of the ellipse at 0°K . To compute the semimajor axis $a = b(1 + \kappa)$ oriented along the [100] axis we used the value $\kappa = 0.77 \times 10^{-2}$ given in^[6].

Apparatus. Figure 5 is a schematic drawing of the apparatus. The required high currents (to 600 A) were obtained from a superconducting transformer in which the secondary winding consisted of a shell 1 and wire 2, both made of lead. The primary winding consisted of 215 turns of niobium-zirconium superconductive wire around a Permalloy core 3. The current I flowing through the central wire was proportional to the current J in the primary winding, which was monitored with the coil 4 connected to a fluxmeter. A copper wire that was also wound around the core 3 carried a 20-Hz alternating current from an acoustic generator for the purpose

of modulating the direct current to a degree that did not exceed the widths of the RFSE lines.

The sample 5 was positioned with respect to the conductor 2 by means of duralumin washers 6 and a bronze spring that pressed the sample from outside (not shown in Fig. 5). The tank-circuit coil of a rf oscillator was clamped against the inside surface of the sample; the turns of this flat spiral coil were parallel to the generating line of the cylinder surface.

The width of the coil winding and its location at the inside surface of the sample (in the [100] direction) were chosen for the purpose of observing the RFSE line corresponding to the strongest RFSE line that was observed by Gantmakher in the case of flat n-state tin samples.^[7]

To permit the observation of undistorted RFSE lines the n-layer adjacent to the oscillator coil had to be of uniform thickness with deviation of only the order of the skin depth, $\delta \sim 10^{-4}$ cm. Therefore in assembling the apparatus we tried to have the axis of the wire 2 coincide with a line through the centers of curvature of the portion of the sample's inside surface that was tangent to the (100) plane. The 6.14-mm diameter washers 6 were prepared with allowance for the contraction of duraluminum when cooled; the deviations for all essential dimensions did not exceed 1μ . Since the softness of lead prevented us from achieving the same accuracy for the lead wire, in the last experiments the part of the wire on which the washers were mounted was made of 3.8-mm diameter niobium. The superconducting niobium-lead junction was made by hot plating of niobium with lead in a vacuum. The rf oscillator operated in the frequency range $f = 3-10$ MHz. We employed the conventional modulating technique for observing the RFSE with automatic plotting of signals proportional to $\partial f / \partial J \sim -\partial X / \partial H$.

3. RESULTS AND DISCUSSION

Examples of $\partial f / \partial J$ plots at different temperatures are shown in Fig. 6. To the right of the minimum associated with the appearance of the n-layer on the sample surface we observe a series of RFSE lines that are associated with many extremal cross sections of the Fermi surface of tin. The positions of these lines can be compared directly with the positions of RFSE lines from flat n-state samples^[7] and with the Fermi-surface model that Weisz^[9] constructed for tin in agreement with experiment.^[7,10] According to this model, the principal parts of the Fermi surface are located in the fourth and fifth zones of the energy spectrum. The fourth zone contains a multiply-connected open surface having large almost cylindrical parts with their axis along [001] and relatively small parts of a complicated cruciform shape. The fifth energy zone contains a multiply-connected open surface consisting of pear-shaped parts connected by tubes. For $H \parallel [001]$ Gantmakher observed six RFSE lines associated with extremal dimensions in the [100] direction. These are primarily central cross sections of a "cylinder" (orbit 1 as in^[7]) and a cruciform surface (orbit 4) in the fourth zone which are shown in Fig. 7. This part of the surface, namely the cross section of the neck of the "cross" (the dashed contour in Fig. 7), evidently produces orbit 15. The maximal (3) and an extremal (2) cross section of the pear-shaped parts of the surface in the fifth zone are responsible for two more RFSE lines.

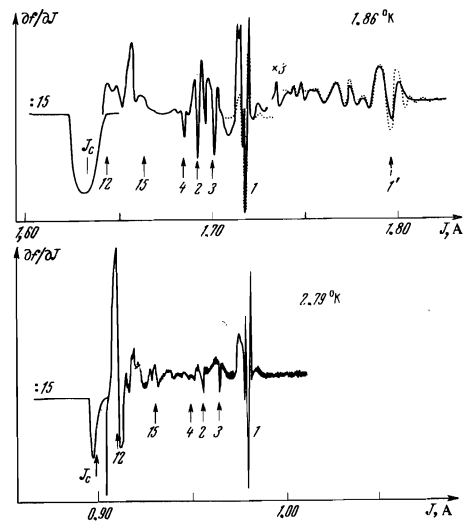


FIG. 6. Experimental traces. The scale of the ordinate axis is arbitrary (and different for the upper and lower curves). The trace of the superconducting transition was produced with diminished sensitivity, but second-order lines were produced with enhanced sensitivity; $f = 3.5$ MHz. The dotted curves designate data in^[8].

The shapes of the corresponding orbits are similar to that shown in Fig. 7 for cross section 1.

The smallest (12) of the considered cross sections evidently belongs to the third or sixth zone, both of which contain small closed parts of the Fermi surface. Orbits 1 and 3 are on convex portions of the Fermi surface and exist over a considerable range of angles ψ between H and [001]; this puts them into the most favorable position for the observation of RFSE in cylindrical layers of metal. For the cross sections 4, 12, and 15, as ψ is increased the measured extremal dimension in the [100] direction is somewhat reduced, although this change is small for angles ψ of the order of tens of degrees. The most intense of all the RFSE lines for tin that were observed in^[7] corresponds to orbit 1.

Because of quite considerable uncertainty about the position of the superconducting transition (J_c') and the absence of a field measuring instrument at the surface of the sample, the positions of all lines were determined relative to the position of the strongest line 1, in accordance with Eq. (1). The calculated positions (shown by arrows in Fig. 6) for lines 1', 3, 2, and 4 are seen to agree well with experiment. The discrepancies for the lines 15 and 12 which appear at higher temperatures are apparently associated with deviations from axial symmetry, which are especially significant for thin n layers, when the n-s boundary is no longer a closed cylinder and emerges at the sample surface. It is therefore difficult to calculate sufficiently accurately the value of J_c' at which the n layers appears.

When the experimental temperature is lowered we distinguish to the right of line 1 a series of oscillations resulting from second order effects (the curve for

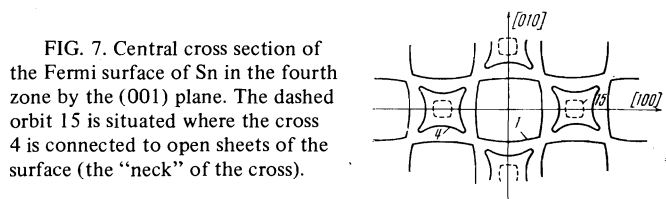


FIG. 7. Central cross section of the Fermi surface of Sn in the fourth zone by the (001) plane. The dashed orbit 15 is situated where the cross 4 is connected to open sheets of the surface (the "neck" of the cross).

1.86° K in Fig. 6). Among these the largest amplitude is exhibited by the second-order line 1' for cross section 1. The position of this line agrees very accurately with a calculation (indicated by an arrow) based on data in [7].

Shapes of RFSE lines. The obtained lines can be compared with ordinary RFSE lines with respect to their shapes as well as their positions. We shall show that lines of orders $m > 1$ are of special interest in this respect.

Let us consider the distribution of an alternating electric field inside and near the surface of the metal. For $d/a \ll 1$ we may neglect the curvature of the n-layer when calculating the distribution of a rf field. We introduce a coordinate system where the plane $z = 0$ coincides with the metal surface and the z axis is directed into the normal metal. The x axis is parallel to H . The distribution of an alternating electric field, $E_\alpha = E_\alpha(z)$ ($\alpha = x, y$) is obtained by solving Maxwell's equations, $\partial^2 E_\alpha / \partial z^2 = -4\pi i \omega c^{-2} j_\alpha$ with the boundary conditions $\partial E_x / \partial z|_0 = 0$ and

$$\partial E_y / \partial z|_0 = -i\omega H \sim / c,$$

where the alternating magnetic field at the metal surface, $H \sim e^{-i\omega t}$, depends on the external conditions and is parallel to the x axis. The current density

$$j_\alpha = -\frac{2|e|\hbar}{(2\pi\hbar)^3} \int v_\alpha(\mathbf{p}) f(\mathbf{p}, z) d\mathbf{p}$$

is determined by solving the kinetic equation for the nonequilibrium supplement f to the Fermi distribution f_0 :

$$f(z, \mathbf{p}) = \frac{|e|\hbar}{\Omega} \frac{\partial f_0}{\partial \varepsilon} \int_{\lambda}^{\circ} \mathbf{v}(\varphi', p_z) \times E \left[z - \frac{1}{\Omega} \int_{\varphi'}^{\circ} v_z(\varphi'') d\varphi'' \right] \exp \left\{ -\frac{\varphi - \varphi'}{\Omega\tau} \right\} d\varphi' \quad (2)$$

$$f_0 = \left(1 + \exp \frac{\varepsilon - \varepsilon_f}{kT} \right)^{-1}.$$

Here we introduce, as is customary, the phase (dimensionless time) of electron motion in a trajectory: $\varphi = \Omega t$, where Ω is the cyclotron frequency for a given orbit (see [1], for example). The integral in (2) is the integral of the scalar product \mathbf{vE} along a trajectory that corresponds to a given state on the Fermi surface which is described by the variables p_x and φ , and passes through a point z . The lower integration limit λ characterizes the instant of collision with the metal surface before the electron enters the given state. We assume diffuse scattering from the surface: $f(0, \mathbf{p})|_{\mathbf{v} > 0} = 0$. For electrons that do not collide with the metal surface we have $\lambda = -\infty$.

For trajectories that intersect the n-s boundary we must take into account the properties of Andreev reflection, which are described by the condition $f(d, \mathbf{p}) = -f(d, -\mathbf{p})$. Hence it is clear that when calculating the integral in (2) we must, upon reaching the n-s boundary, go over to the trajectory for the state that is symmetric with respect to the center of the Brillouin zone (Fig. 8), by reversing the sign of the charge before the integral but leaving the sign of Ω unchanged. However, this can be conceived somewhat differently. The part of the trajectory between the points a and b (the dashed curve on the right side of Fig. 8) and the virtual part of the closed trajectory between b and a for $z > d$ are symmetric with respect to the point of reflection. Therefore, to calculate the integral in (2), when the n-s boundary is

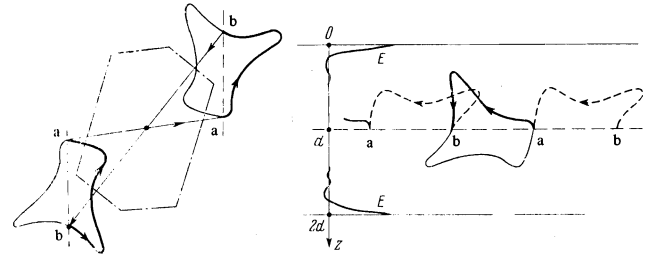


FIG. 8. Cross section of a part of the Fermi surface (left), and the corresponding quasiparticle trajectory (right).

crossed we do not have to reverse the signs of the velocity \mathbf{v} and the charge if we assume $E(z) = E(2d - z)$.

Thus the problem of the field distribution in the n-layer $0 \leq z \leq d$ is equivalent to that of the field distribution in a plate $0 \leq z \leq 2d$ subject to the condition $E(z) = E(2d - z)$.

The field distribution and the dependence on H of the surface impedance of the plate:

$$Z = \frac{4\pi i \omega}{c^2} \frac{E_y(z)|_{z=0}}{\partial E_y / \partial z} \quad (3)$$

were computed by Juras [11] for spherical and cylindrical Fermi surfaces in the cases of both symmetric excitation, $E_y(0) = E_y(2d)$, and antisymmetric excitation, $E_y(0) = -E_y(2d)$, and the experimental curves for tin reveals, however, that we cannot justifiably substitute a section of simple geometric shape for a complicated Fermi surface. First, the theoretical curves of $\partial X / \partial H$ are considerably broader than the experimental curves. Furthermore, a comparison with experiment for the orientation $H \parallel [001]$ in tin is rendered difficult because the cylindrical part of the Fermi surface in the fourth zone is slightly undulating and has maximal and minimal diameters that are close in magnitude, thus complicating the line shape. It must also be mentioned that some fine effects, such as the splitting of the left-hand maximum of line 1, were not observed in all the experiments. This situation can possibly be associated with nonreproducible irregularities of the n-s boundary.

It was possible to compare our curves more closely with the RFSE lines in Gantmakher's experiments [7, 8] when the sample was placed within the tank-circuit coil, i.e., when the conditions for the antisymmetric excitation, $E_y(0) = -E_y(2d)$, were satisfied. As in those experiments, the measured signal was proportional to the change ΔX . Because of the boundary condition $H_y(0) = \text{const}$, this means that changes in the reactive component of the electric field at the metal surface, $\Delta E_y(0)$, were being recorded. This quantity can be represented as the sum of two terms: $\Delta E_y(0) = \Delta E_1 + \Delta E_2$, where ΔE_1 is the change of the field that would occur if the surface $z = 2d$ were not subjected to an external field, and ΔE_2 is the change of the field at $z = 0$ because of the external field applied at $z = 2d$. It is obvious that ΔE_2 has opposite signs for antisymmetric and symmetric excitation, whereas ΔE_1 is independent of the kind of excitation.

For a second-order line in the case of skin depth $\delta \ll d$ it can be assumed, on the basis of calculations given in [1], that $\Delta E_1 / \Delta E_2 \approx e^{-\alpha d / l} \sqrt{\delta / d}$, where αd is the length of the section of the trajectory between $z = 0$ and $z = 2d$ ($\alpha \gtrsim 1$). In this case ΔE_1 can be neglected as compared with ΔE_2 , because $\delta / d \sim 10^{-2}$ and $d \approx l$. Consequently, for $m > 1$ the RFSE lines in an n-layer of thickness d bounded by the s-phase should agree in

shape with RFSE lines in plates of thickness $2d$ when the sign of the ordinate is reversed. For $m = 1$, when the "cutting off" of trajectories plays an important role in the RFSE, the ratio $\Delta E_1/\Delta E_2 \approx e^{-\alpha d/l}$ (see^[11]) is not so small and line-shape differences can be observed that are not attributable merely to a change of sign. The dotted traces in Fig. 6 are "inverted" experimental traces of the corresponding portions of the $\partial f/\partial H$ curves in^[8]. The axial scales were chosen in accordance with the positions and heights of the peaks for lines 1 and 1'. The agreement of the curves between lines 1 and 1' confirms the foregoing statements relating the RFSE to chains of trajectories. When compared for opposite signs the shapes of the lines 1 agree less well; this result is accounted for by the cutting-off effect. Thus, both the positions and the shapes of RFSE lines confirm Andreev's hypotheses concerning the reflection of excitations from the boundary between the superconducting and normal phases.

It should be noted that our experiments differ from those of Gantmakher with regard to the relative amplitudes of the principal line and the lines observed in multiples of the initial field. Although the differences in the relative amplitudes of lines 4, 2, and 3 can be attributed to a reduction of the d/l ratio, for lines 1 and 1' the observed difference is only aggravated by taking the change of d/l into account; to obtain line traces in multiples of the field with the same relative amplitudes, the sensitivity used in Gantmakher's experiments would have to be about three times greater than in our case. In turn, we did not observe the $d = 3D/2$ line with a signal-noise ratio ≈ 10 , although in Gantmakher's work the lines in $2H_0$ and $3H_0$ fields differ by a factor of as much as three. The foregoing facts are evidence that in the n -layer RFSE lines determined by the condition $d = mD/2$ with odd m are attenuated relative to those with even m . The difference in intensity is probably associated with the fact that for odd m at each return to the skin layer the particles are shifted parallel to the sample axis through a distance equal to the trajectory diameter, but that for even m the particles return to the same point of the sample surface. It is evident that surface irregularities have a stronger influence in the first case, making it difficult for particles to return repeatedly to the skin layer.

Measurement of electron mean free paths. As we know, the RFSE in normal metal plates can be used to measure electron mean free paths (see^[11], for example), because electron scattering makes the line amplitude A depend on the ratio S/l , where S is the path length between two successive passages of an electron through the skin layer. In our experiments S is varied together with the n -layer thickness d at which a line is observed, by changing the sample temperature and thereby varying

the critical field H_C . Then $S = \alpha d$, where α is determined by the shape of the given orbit.

According to (1), when a line is observed we have in first approximation $d \sim H_C^{-1}$. Therefore for $T \lesssim T_C$ small changes of T , which have little effect on the magnitude of l , can lead to considerable changes in the magnitude of d and therefore of the RFSE line amplitudes. We plotted the temperature dependence of the amplitude A for $T \geq 1.3^\circ$ in the cases of all first-order RFSE lines except line 12, the observation of which for $T < 2.8^\circ$ was impeded by broadening of the superconducting transition line. For $T \gtrsim 3.2^\circ$ the amplitudes fell below the noise level even in the cases of the strongest lines, 1 and 12.

Knowing the function $H_C(T)$ and the extremal orbit dimensions, we obtain a relation between temperature and the layer thickness d at the instant when a line is observed; this relation is used to convert the function $A(T)$ to the form $A(d)$. Figure 9 shows some logarithmic plots of this experimental dependence. With the exception of line 1, the shapes of all lines are practically independent of temperature. For line 1, A was taken to be the ordinate distance between the principal minimum and the right-hand maximum of the $\partial f/\partial J$ trace. If we neglect multiple returns of electrons to the skin layer, the line amplitudes should depend on d/l as $e^{-\alpha d/l}$. Figure 9 shows that straight lines fit satisfactorily the experimental values of $\ln A(d)$. It follows that repeated returns of electrons to the skin layer actually played no part in our experiments; moreover, the mean free path did not change substantially with temperature. Such repeated returns were apparently excluded not only because the mean free path was usually considerably smaller than the length of the trajectory, but also because for odd m , as already mentioned, the return of an electron to the surface was shifted along the surface.

Using data for orbit shapes in^[9], we took $\alpha = 4$ for the cross sections 1, 2, 3, and 15; $\alpha = 4.4$ for cross section 4; and $\alpha = 3.2$ for line 12, assuming that it corresponds to the cross section of the surface in the third zone. With these values of α the slopes of the straight lines in Fig. 9 correspond to $l \approx 0.5$ mm for cross section 1; $l \approx 0.12$ mm for cross sections 2, 3, 4, and 15; and $l \approx 0.04$ mm for cross section 12.

The values obtained for l are understood to be the electrons' residual mean paths which were determined by impurities and lattice defects in our samples. A comparison of the l values for different cross sections can be of objective interest. The differences between the values of l for cross sections 1 and 12 and those of the other cross sections undoubtedly lie outside the limits of the possible errors.

For line 1, which was investigated in the broadest range (1–3.5) of the ratio S/l , changes of shape were observed. With decreasing temperature, the left-hand maximum grew considerably faster than the right-hand maximum; the dependence $A(d)$ could not be described by a simple exponential. This effect could possibly result from cutting-off, which should be manifested more strongly for small S/l . The dependence on d/l exhibited in our experiments by the shape of the RFSE line 1 agrees qualitatively with theoretical calculations. It was shown in^[11] that as d/l decreases the first peak of RFSE lines should grow considerably faster than the following peaks.

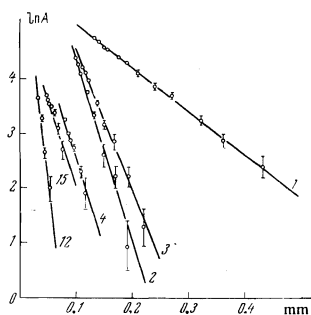


FIG. 9. Dependence of RFSE line amplitudes (in arbitrary units) on n -layer thickness.

4. CONCLUSION

It can be stated, in conclusion, that the investigation of the RFSE in a layer of normal metal bounded by its superconducting phase and a vacuum has directly demonstrated the peculiar character of electron reflection from the n-s boundary. It has also revealed additional opportunities for studying the electronic structure of a normal metal, such as measurements of the diameters of small Fermi-surface cross sections and measurements of electron mean free paths in different extremal cross sections. A logical continuation of the study of Andreev reflection would be an attempt to observe the penetration of excitations through the n-s boundary into the superconducting phase, followed by similarly performed observation from the other side.

However, calculations have shown that to accelerate carriers to energies $\epsilon \gtrsim \Delta$ such large electric fields would be required that the Joule losses would exceed all permissible levels. This fundamental obstacle could apparently be avoided by accelerating the necessary group of electrons in a small region near a very fine microjunction, or by employing selective absorption of electric field energy under cyclotron resonance conditions. Observations at uhf would possess the advantage of permitting one to measure both the probability that

excitations cross the n-s boundary and the propagation velocity of the excitations in the superconducting phase.

- ¹E. A. Kaner and V. F. Gantmakher, *Usp. Fiz. Nauk* **94**, 193 (1968) [*Sov. Phys.-Usp.* **11**, 81 (1968)].
- ²I. P. Krylov and Yu. V. Sharvin, *ZhETF Pis. Red.* **12**, 102 (1970) [*JETP Lett.* **12**, 71 (1970)].
- ³A. F. Andreev, *Zh. Eksp. Teor. Fiz.* **46**, 1823 (1964) and **51**, 1510 (1966) [*Sov. Phys.-JETP* **19**, 1228 (1964) and **24**, 1019 (1967)].
- ⁴Handbook of Physics and Chemistry, C. D. Hodgman ed., Chemical Rubber Publishing Co., Cleveland, Ohio, 37th ed., 1955-1956, p. 2063.
- ⁵G. K. White, *Phys. Lett.* **8**, 294 (1964).
- ⁶V. B. Zernov and Yu. V. Sharvin, *Zh. Eksp. Teor. Fiz.* **36**, 1038 (1959) [*Sov. Phys.-JETP* **9**, 737 (1959)].
- ⁷V. F. Gantmakher, *Zh. Eksp. Teor. Fiz.* **44**, 811 (1963) [*Sov. Phys.-JETP* **17**, 549 (1963)].
- ⁸V. F. Gantmakher, *Zh. Eksp. Teor. Fiz.* **43**, 345 (1962) [*Sov. Phys.-JETP* **16**, 247 (1963)].
- ⁹G. Weisz, *Phys. Rev.* **149**, 504 (1966).
- ¹⁰J. E. Craven and R. W. Stark, *Phys. Rev.* **168**, 849 (1968).
- ¹¹G. E. Juras, *Phys. Rev.* **187**, 784 (1969).

Translated by I. Emin

104